Ruthenium(III) Complexes with a Phenolate-O, Imine-N, and Amide-O Coordinating Ligand: Syntheses, Structures, Properties, and Protonation Studies of Coordinated Amide

Satyanarayan Pal,[a] and Samudranil Pal*[a]

Keywords: Ruthenium / Acetylhydrazone / Crystal structures / Protonation / Redox chemistry

The reaction of *cis*-[$RuCl_2(dmso)_4$], *N*-(acetyl)-*N′*-(salicylidene)hydrazine (H_2acs), and KOH (1:2:2 molar ratio) in methanol under aerobic conditions produces a ruthenium(III) complex, [Ru(acs)(Hacs)]·H_2O. Addition of one mol equivalent of $HClO_4$ to this complex in methanol affords [$Ru(Hacs)_2$]ClO_4. On the other hand, reaction of one mol equivalent of KOH with [Ru(acs)(Hacs)]·H_2O in methanol produces K[$Ru(acs)_2$]. All three complexes have been characterised by elemental analyses, magnetic, spectroscopic, and electrochemical techniques. In solution, except for [Ru(acs)(Hacs)]·H_2O, the other two complexes are 1:1 electrolytes. Solid state magnetic moments (at 298 K) of the complexes are in the range 1.91–2.15 μ_B. These values reflect a spin state $S = 1/2$ and hence low-spin ruthenium(III) within each complex is observed. X-ray structures of [Ru(acs)(Hacs)]·H_2O and the tetraphenylphosphonium salt of [$Ru(acs)_2$]$^-$ have been determined. In both complexes, the ligands bind to the metal ion meridionally through the phenolate-O, the imine-N and the amide-O atoms. In [Ru(acs)(Hacs)]·H_2O, the amide functionality of one of the ligands is protonated, and in [PPh_4][$Ru(acs)_2$] the amide functionalities of both ligands are deprotonated. Electronic spectra of the complexes display ligand-to-metal charge-transfer bands in the range 626–699 nm. Cyclic voltammetry reveals a $Ru^{III} \rightarrow Ru^{IV}$ oxidation change in the potential range of 0.56–0.84 V (vs. SCE) for these complexes. The charge-transfer band positions and the oxidation potentials are significantly influenced by the protonation state of the O-coordinating amide functionality present in each ligand. The pK_a values of the coordinated amide functionalities have been determined by spectrophotometric titration.

Introduction

The interest in ruthenium chemistry stems from its ability to have a wide range of oxidation states (−2 to +8) and various coordination geometries. Due to these characteristics complexes of ruthenium exhibit versatile electron-transfer properties and hence a wide range of reactivities.[1]

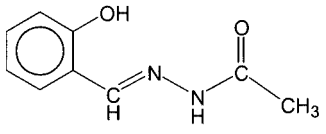

H_2acs

As a result a large variety of ruthenium complexes have been utilized in studies on artificial photosynthesis, photomolecular devices, elucidation of structural and electron-transfer properties of proteins and DNA, catalytic oxidation of water and organic substrates and stoichiometric as well as catalytic reactions for organic synthesis.[1l−1t] Due to such a broad array of applications there is a continuous pursuit for new complexes of ruthenium with diverse types of ligands. The primary objective is to tune the properties of the complex by alteration of the coordination geometry and the nature of the coordinating functionalities. Recently we have reported a series of ruthenium(II) bis complexes with a tridentate pyridine-N, imine-N, and amide-O donor deprotonated Schiff-base system, *N*-(aroyl)-*N′*-(picolinylidene)hydrazines.[2] In these complexes, the energy separation between the metal-dπ and ligand-π* level remains constant regardless of the variation in the polar effect of the substituent on the aroyl fragment of the ligand. In this report, we have explored the coordination chemistry of ruthenium with a similar kind of Schiff base *N*-(acetyl)-*N′*-(salicylidene)hydrazine (H_2acs, the two H′s representing the dissociable phenolic and amide protons). In the deprotonated state the Schiff base acs^{2-} can coordinate to a metal ion via the phenolate-O, the imine-N, and the deprotonated amide-O atoms forming a six- and a five-membered chelate ring. This type of coordination mode by acs^{2-} and similar ligands is known.[3] The reasons for the choice of this Schiff base are as follows: it contains high oxidation state promoting[4] phenolic hydroxy and amide functionalities; the O-coordinating amide functionality provides a rare opportunity to study the influence of the amide protonation state on the coordination geometry and physical properties of the complex, which is not easy for amide-N coordinated species. Herein, we describe three new ruthenium(III) bis-chelates with H_2acs. These complexes differ only in the protonation state

[a] School of Chemistry, University of Hyderabad, Hyderabad 500 046, India
Fax: (internat.) +91-40/2301-2460
E-mail: spsc@uohyd.ernet.in

  DOI: 10.1002/ejic.200300232

of the coordinated amide functionalities. Solid state molecular structures for two of these three complexes have been determined by X-ray crystallography In solution, dependence of the spectral and the redox features on the amide protonation state has been scrutinized.

Results and Discussion

Syntheses and Characterisation of the Complexes

The neutral complex [Ru(acs)(Hacs)] was isolated from a methanolic medium by reacting *cis*-[$RuCl_2(dmso)_4$], H_2acs and KOH in 1:2:2 molar ratio under aerobic conditions. The monohydrated complex precipitates from the reaction mixture as a green solid in reasonable yield. Atmospheric oxygen is the most likely oxidizing agent in the oxidation of the metal ion during the formation of the complex. If the stoichiometrically required molar ratio (1:2:3) is taken, the amount of the precipitated complex is significantly lower. However, the potassium salt of the anionic complex $[Ru(acs)_2]^-$ can be recovered from the filtrate. The dissociation of the phenolic-OH proton may happen in the absence of a strong base like OH^-. Most likely for this reason the 1:2:2 mol ratio gives a better yield of the neutral complex and for stoichiometric mol ratio (1:2:3) formation of $[Ru(acs)_2]^-$ has been observed. A more convenient and clean method for the synthesis of $K[Ru(acs)_2]$ is the treatment of [Ru(acs)(Hacs)]·H_2O with one molar equivalent of KOH in methanol. By using a similar approach the perchlorate salt of the cationic complex $[Ru(Hacs)_2]^+$ can be prepared by reacting [Ru(acs)(Hacs)]·H_2O and $HClO_4$ in a 1:1 molar ratio in methanol. The elemental analysis data (Table 1) for all three complexes agree with the proposed molecular formulae. Molar conductivity values (Table 1) of the complexes in solutions are consistent with the neutral character of [Ru(acs)(Hacs)]·H_2O and 1:1 electrolyte nature[5] of both $K[Ru(acs)_2]$ and $[Ru(Hacs)_2]ClO_4$. The solid-state magnetic moments (Table 1) of these complexes at 298 K are in the range 1.91−2.15 μ_B. Thus, in each complex, the ruthenium centre is in the +3 oxidation state and is low-spin in character.

Spectral Characteristics

The infrared spectra of [Ru(acs)(Hacs)]·H_2O and $[Ru(Hacs)_2]ClO_4$ display multiple peaks in the range 3206−2710 cm^{-1}. These peaks are most likely associated with the N−H group of the protonated amide functionalities in these complexes.[6a] On the other hand, absence of any such peak in this region of the spectrum of $K[Ru(acs)_2]$ confirms deprotonation of the amide functionalities in both ligands. In addition to the above mentioned peaks, [Ru(acs)(Hacs)]·H_2O displays a broad peak centred at 3427 cm^{-1} ascribable to the lattice water molecules.[6b] All three complexes display three medium to strong peaks at about 1597, 1550 and 1520 cm^{-1}. These peaks are possibly due to the metal-coordinated azomethine and protonated/deprotonated amide functionalities of the ligands.[2,3,6a] The presence of perchlorate ion in $[Ru(Hacs)_2]ClO_4$ is indicated by a broad and strong peak at ca. 1100 cm^{-1} and a sharp peak at ca. 620 cm^{-1}.

The electronic spectroscopic data of the complexes in acetonitrile solutions are listed in Table 1. The spectral profiles are quite similar. In the visible region, the major features displayed by these complexes are a band in the range 626−699 nm and a shoulder within the range 487−504 nm (Table 1). These absorptions are assigned to the phenolate-pπ to the metal-dπ charge-transfer transitions.[7] Interestingly, $[Ru(Hacs)_2]ClO_4$, where both the amide functionalities of the ligands are protonated, displays the first band at lower energy (699 nm) whereas the completely deprotonated species $K[Ru(acs)_2]$ displays the same band at higher energy (626 nm). The band position shift suggests that the energy gap between the phenolate-pπ and the metal-dπ levels is significantly decreased due to the protonation of the O-coordinating amide functionalities of the two ligands. The band position of the neutral complex [Ru(acs)(Hacs)], where only one amide functionality is protonated, shows the same trend but to a much smaller extent. The strong absorptions (Table 1) observed in the ultraviolet region of the spectra are most likely due to transitions involving only ligand orbitals.

The EPR spectra of the complexes in frozen (103 K) methanol/toluene (1:1) solutions are very similar. A representative spectrum is shown in Figure 1. Each of them display three distinct signals (Table 2) indicating the distortion of the N_2O_4 coordination sphere around the metal centre from octahedral symmetry. This distortion can be measured in terms of axial (Δ) and rhombic (V) components. The axial distortion (Δ) splits t_2 into "a" and "e" and the rhombic component again splits "e" into nondegenerate

Table 1. Elemental analysis,[a] molar conductivity, magnetic moment[b] and electronic spectral[c] data

Compound	%C	%H	%N	Λ_M (Ω^{-1} cm^2 M^{-1})	μ_{eff}/μ_B	λ_{max} nm ($\varepsilon/10^3$ M^{-1} cm^{-1})
[Ru(acs)(Hacs)]·H_2O	45.53 (45.76)	3.87 (4.05)	11.63 (11.86)	15[d]	1.91	630 (1.1), 504[e] (1.2), 375 (15.4), 343 (15.5), 271[e] (19.6)
$[Ru(Hacs)_2]ClO_4$	38.61 (38.96)	3.42 (3.27)	9.85 (10.10)	117[f]	2.15	699 (2.0), 496[e] (1.1), 365 (13.6), 267 (18.6), 235 (26.1)
$K[Ru(acs)_2]$	43.58 (43.90)	3.13 (3.27)	11.04 (11.37)	138[f]	2.01	626 (0.7), 487[e] (1.2), 380 (14.7), 342 (16.4), 282[e] (15.6), 241 (28.3)

[a] Calculated values are in parentheses. [b] In powder phase at 298 K. [c] In CH_3CN solvent. [d] In $HCON(CH_3)_2/CH_3CN$ (1:4) solvent. [e] Shoulder. [f] In CH_3CN solvent.

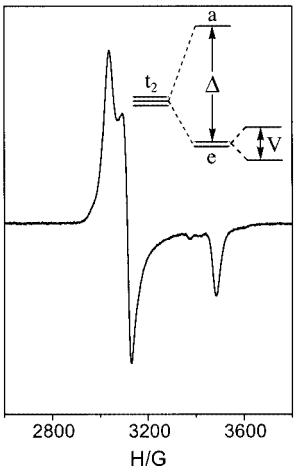

Figure 1. EPR spectrum of $[Ru(Hacs)_2]ClO_4$ in frozen (103 K) methanol/toluene (1:1) solvent mixture and t_2 splitting pattern

Table 2. EPR *g*-values,[a] calculated distortion parameters and near-IR transitions[b]

Compound	g_1	g_2	g_3	Δ/λ	V/λ	$\Delta E_1/\lambda$	$\Delta E_2/\lambda$
$[Ru(acs)(Hacs)]\cdot H_2O$	2.186	2.133	1.876	4.849	−0.935	4.377	5.659
$[Ru(Hacs)_2]ClO_4$	2.166	2.114	1.888	5.069	−1.064	4.540	5.921
$K[Ru(acs)_2]$	2.208	2.161	1.854	4.492	−0.670	4.125	5.225

[a] In 1:1 methanol/toluene at 103 K. [b] The calculations are based on spin-orbit coupling constant (λ) = 1000 cm^{-1}.

components (Figure 1). In addition to Δ and V, spin-orbit coupling also influences the extent of the energy gaps between these levels. Thus, two ligand-field transitions of energies ΔE_1 and ΔE_2 ($\Delta E_1 < \Delta E_2$) are possible within these three levels. The distortion parameters and the transition energies have been quantified using the observed *g* values and the *g* tensor theory of low-spin d^5 complexes (Table 2).[8] The distortion parameters suggest that the axial component is significantly larger than the rhombic component in all of the complexes. The ΔE_1 and ΔE_2 transitions are expected to occur in the range 4100−4600 and 5200−6000 cm^{-1} (Table 2), respectively. No absorption was detected in either of the above two regions due to non-transparency of the solvent. Similar EPR spectral profiles and the comparable values of the distortion parameters calculated from the EPR data indicate that the nature and extent of distortions from the octahedral geometry are not very different in these complexes. Thus there is no significant change in the distortion pattern of the N_2O_4 coordination sphere around the low-spin ruthenium(III) centre due to protonation or deprotonation of the amide functionalities of the ligands. Earlier we reported a similar series of three high-spin iron(III) complexes with enolate-O, imine-N, and amide-O donor deprotonated acetylacetone benzoylhydrazone. It may be noted that unlike the present series of complexes, the variation of the protonation state of the amide functionalities changes the distortion pattern from rhombic to near-axial in the iron(III) complexes.[3b]

Description of Structures

The solid-state molecular structure of $[Ru(acs)(Hacs)]\cdot H_2O$ has been determined by X-ray crystallography. The complex crystallises in the *C*2/*c* space group. The structure of the complex molecule is depicted in Figure 2. The bond parameters associated with the metal centre are listed in Table 3. Each ligand binds the metal ion meridionally through the phenolate-O, the imine-N, and the amide-O atoms forming a six- and a five-membered chelate ring. Two ligands are related by a crystallographically imposed twofold axis of symmetry passing through Ru and bisecting the angles O1−Ru−O1′ and O2−Ru−O2′ (Figure 2). The presence of this twofold axis of symmetry indicates that two ligands are crystallographically equivalent. This could also indicate that both ligands are chemically equivalent. Taking into account the neutral character of the complex, this will be possible if the oxidation state of the metal centre is +2 and the ligands are monoanionic ($Hacs^-$). Considering the more acidic character of the phenolic-OH the amide functionality in each ligand has to be protonated. The second possibility is that the oxidation state of the metal centre is +4 and the ligands are dianionic (acs^{2-}). However, the physical properties (vide supra) of the complexes clearly

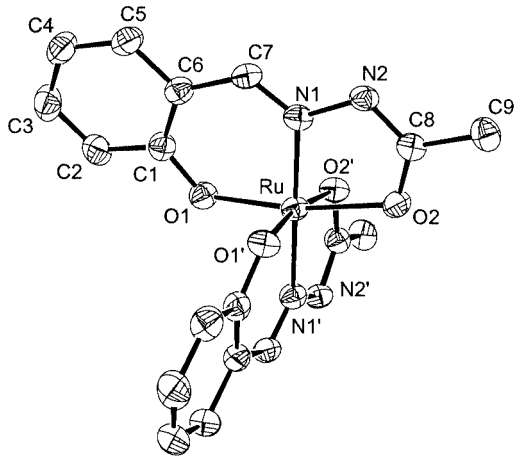

Figure 2. The structure of [Ru(acs)(Hacs)] showing the 35% probability thermal ellipsoids and the atom-labelling scheme; hydrogen atoms are omitted for clarity

Table 3. Selected bond lengths (Å), and angles (°) for $[Ru(acs)(Hacs)]\cdot H_2O$[a]

Ru−O(1)	1.961(2)	Ru−O(1)′	1.961(2)
Ru−N(1)	1.983(3)	Ru−N(1)′	1.983(3)
Ru−O(2)	2.063(2)	Ru−O(2)′	2.063(2)
O(1)−Ru−O(1)′	95.12(14)	O(1)−Ru−O(2)	169.57(9)
O(1)−Ru−O(2)′	90.46(11)	O(1)−Ru−N(1)	93.16(9)
O(1)−Ru−N(1)′	87.45(9)	O(1)′−Ru−O(2)	90.46(11)
O(1)′−Ru−O(2)′	169.57(9)	O(1)′−Ru−N(1)	87.45(9)
O(1)′−Ru−N(1)′	93.16(9)	O(2)−Ru−O(2)′	85.45(14)
O(2)−Ru−N(1)	78.27(10)	O(2)−Ru−N(1)′	101.06(9)
O(2)′−Ru−N(1)	101.06(9)	O(2)′−Ru−N(1)′	78.27(10)
N(1)−Ru−N(1)′	179.11(13)		

[a] Symmetry transformation used to generate equivalent atoms: $-x, y, -z + 1/2$.

suggest a +3 oxidation state of the metal ion in all of the complexes. In addition, the observed (Table 3) Ru−O(phenolate) and Ru−N(imine) distances are similar to the distances reported for Ru^{III} complexes with ligands that provide the deprotonated salicylaldimine or similar moiety for metal ion binding.[9] The significantly shorter Ru−O(amide) distance compared to the distances observed in ruthenium(II) complexes[2] containing the same coordinating atom is also consistent with the +3 oxidation state of the metal ion. Thus the two ligands are not chemically equivalent, one of them is dianionic acs^{2-} and the other one is monoanionic $Hacs^{-}$. The origin of the crystallographic equivalence of the two ligands is therefore due to either a static disorder resulting from the crystallographic superposition of an equal number of $Hacs^{-}$ and acs^{2-}, or a dynamic disorder due to rapid (on the crystallographic time scale) H-atom transfer between the two amide-N centres. Rapid H-atom transfer in the solid state is highly unlikely to occur and hence the observed crystallographic equivalence of the two ligands can be attributed solely to a static disorder. The lattice water molecule is also similarly disordered and the O-atom sits at a special position with half occupancy. The distance (2.754 Å) between the amide-N atom (N2) and the water O-atom suggests an N−H···O hydrogen bonding interaction. Due to disorder the amide-N atoms of both ligands show the same interaction. In the crystal lattice, a one-dimensional chain of an alternating complex molecule and a water molecule is formed via this hydrogen bonding. The H_2O hydrogen atoms are also involved in inter-chain weak H-bonding interactions with the amide-O and phenolate-O atoms (O−H···O distances are 3.370 and 3.250 Å, respectively) forming a two-dimensional network of $[Ru(acs)(Hacs)]\cdot H_2O$ in the crystal lattice (Figure 3).

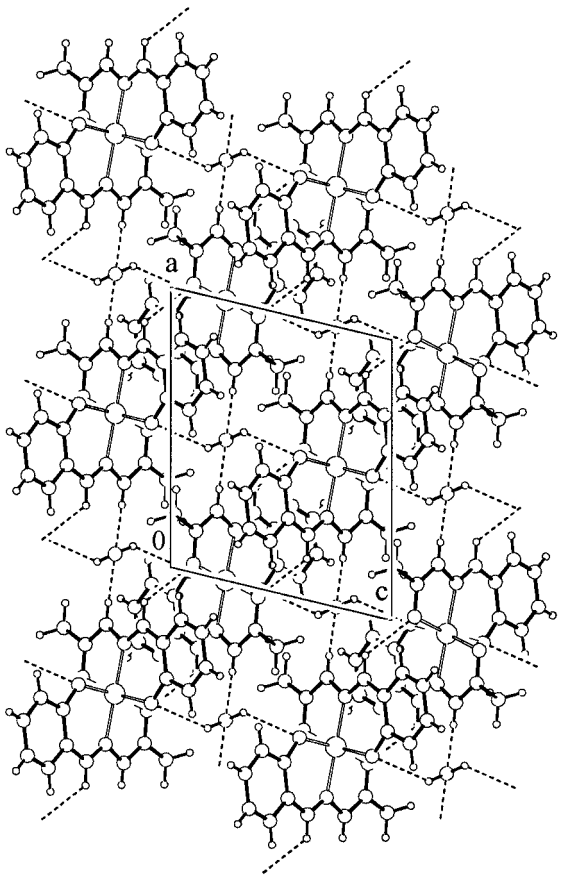

Figure 3. Two dimensional network of $[Ru(acs)(Hacs)]\cdot H_2O$ along *b* axis

We were unable to grow X-ray quality single crystals of $K[Ru(acs)_2]$. However, the tetraphenylphosphonium salt of $[Ru(acs)_2]^{-}$ crystallises in the $P\bar{1}$ space group. Single crystals of $[PPh_4][Ru(acs)_2]$ were obtained by the reaction of $K[Ru(acs)_2]$ and PPh_4Cl in acetonitrile followed by addition of toluene and slow evaporation of the mixture in air. The asymmetric unit contains a PPh_4^{+} cation, a complex anion $[Ru(acs)_2]^{-}$, and a toluene molecule that has been located at two sites. The structure of $[PPh_4][Ru(acs)_2]$ is shown in Figure 4 and selected bond parameters involving the metal centre are collected in Table 4. As in the previous structure the ligands bind the metal ion meridionally. The Ru−O(amide), Ru−O(phenolate) and Ru−N(imine) distances are typical for a ruthenium(III) species.[2,9] These distances clearly indicate that there is essentially no difference with respect to the binding strength of the two ligands. The dianionic nature of both ligands and hence the single negative charge on the complex and the +3 oxidation state of the metal ion are further confirmed by the presence of the PPh_4^{+} ion. The bond parameters of the cation are unexceptional.[10]

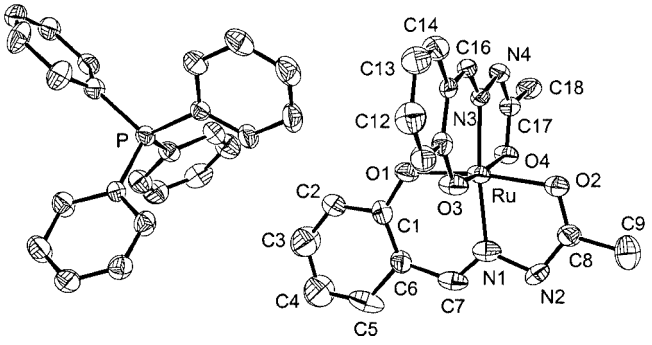

Figure 4. Structure of $[PPh_4][Ru(acs)_2]$ with the atom-labelling scheme; all atoms are represented by their 25% probability thermal ellipsoids; the labelling of the carbon atoms in the cation and hydrogen atoms are not shown for clarity

In contrast to $[Ru(acs)(Hacs)]\cdot H_2O$, there are no good, conventional hydrogen-bond acceptors or donors in $[PPh_4][Ru(acs)_2]\cdot C_6H_5CH_3$. However, this species also forms a two-dimensional network in the crystal lattice via several C−H···π interactions.[11] The H···centroid distances and the C−H···centroid angles are within the ranges 2.742−3.177 Å and 134.98−169.48°, respectively. The methyl group C-H, the aromatic C-H of the ligand and that of the phenyl groups of the cation are involved in these interactions with the π-electrons of the toluene, PPh_4^{+} phenyl groups, ligand phenolate ring and the chelate rings. A few of these interactions are depicted in Figure 5.

Table 4. Selected bond lengths (Å), and angles (°) for $[PPh_4][Ru(acs)_2]\cdot C_6H_5CH_3$

Ru−O(1)	1.971(7)	Ru−O(2)	2.021(7)
Ru−O(3)	1.975(7)	Ru−O(4)	2.024(6)
Ru−N(1)	2.020(9)	Ru−N(3)	1.999(7)
O(1)−Ru−O(2)	171.7(3)	O(1)−Ru−O(3)	92.5(3)
O(1)−Ru−O(4)	90.4(3)	O(1)−Ru−N(1)	95.2(3)
O(1)−Ru−N(3)	90.9(3)	O(2)−Ru−O(3)	90.4(3)
O(2)−Ru−O(4)	87.7(3)	O(2)−Ru−N(1)	77.1(3)
O(2)−Ru−N(3)	96.6(3)	O(3)−Ru−O(4)	172.1(3)
O(3)−Ru−N(1)	87.8(3)	O(3)−Ru−N(3)	93.9(3)
O(4)−Ru−N(1)	99.3(3)	O(4)−Ru−N(3)	78.7(3)
N(1)−Ru−N(3)	173.6(4)		

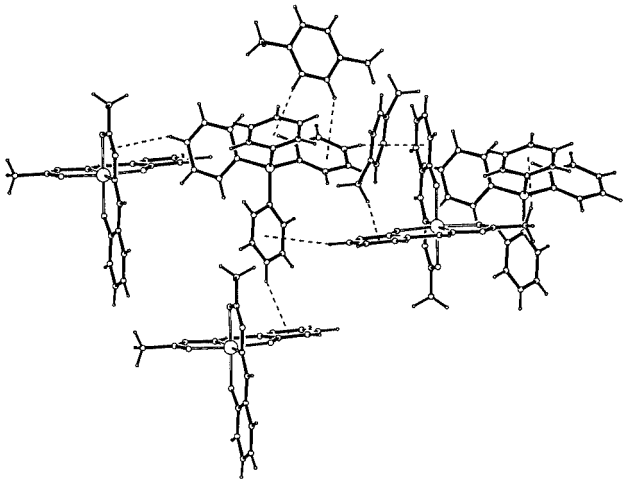

Figure 5. Various C−H···π interactions in the crystal lattice of $[PPh_4][Ru(acs)_2]\cdot C_6H_5CH_3$

Electrochemical Properties

Electron transfer properties of the complexes in acetonitrile/dimethylformamide (9:1) solutions (0.1 M TBAP) have been investigated with the help of cyclic voltammetry. Each of the three complexes displays an oxidation response on the anodic side of SCE (Figure 6). The one-electron stoichiometry for these oxidation processes is ascertained by comparing the current heights with known one-electron redox processes under identical conditions.[2,9a] The anionic complex $[Ru(acs)_2]^-$ has the lowest potential ($E_{1/2}$ = 0.56 V and ΔE_p = 70 mV)[12] and the cationic complex $[Ru(Hacs)_2]^+$ has the highest potential ($E_{1/2}$ = 0.84 V and ΔE_p = 150 mV). The potential ($E_{1/2}$ = 0.76 V and ΔE_p = 240 mV) for the neutral complex [Ru(acs)(Hacs)] is in between the above two values. The free Schiff base H_2acs shows an irreversible oxidation with comparatively much higher current at +1.38 V under identical conditions. Thus the oxidation responses observed for the complexes are assigned to the $Ru^{III} \rightarrow Ru^{IV}$ process. The trend in the $E_{1/2}$ values indicates that the oxidation of the metal centre in the anionic complex where the amide functionality for each of the two ligands is deprotonated, is most favourable, and that in the cationic complex where the amide functionalities are protonated, is most difficult. This behaviour is likely to be primarily due to electrostatic reasons.

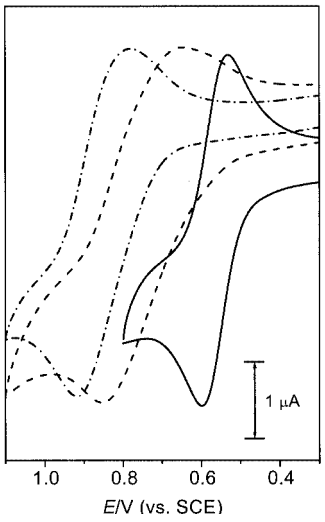

Figure 6. Cyclic voltammograms of $K[Ru(acs)_2]$ (−), $[Ru(acs)(Hacs)]\cdot H_2O$ (-----), and $[Ru(Hacs)_2]ClO_4$ (−·−·−) in acetonitrile/dimethylformamide (9:1) solvent mixture (0.1 M TBAP) at scan rates of 50 mV s^{-1}

On the cathodic side of the SCE, both $K[Ru(acs)_2]$ and [Ru(acs)(Hacs)] display a reduction response. The $E_{1/2}$ values are −1.11 V (ΔE_p = 80 mV) and −1.13 V (ΔE_p = 80 mV), respectively. In both cases, the anodic (i_{pa}) and cathodic (i_{pc}) peak currents are very similar to the current heights observed for the $Ru^{III} \rightarrow Ru^{IV}$ processes. On the other hand, $[Ru(Hacs)_2]ClO_4$ displays three reduction responses at $E_{1/2}$ = −0.20 V (ΔE_p = 100 mV), E_{pc} = −0.90 and −1.63 V. For the highest potential reduction i_{pc} is much larger than the i_{pa}. However, the i_{pc} is similar to that of the $Ru^{III} \rightarrow Ru^{IV}$ process. This first reduction response of $[Ru(Hacs)_2]ClO_4$ and the reduction responses observed for [Ru(acs)(Hacs)] and $K[Ru(acs)_2]$ may be assigned to the $Ru^{III} \rightarrow Ru^{II}$ process and the differences in the potential values can be rationalised considering the electrostatic effect. However, the trend in the reduction potential values is significantly different than that of the oxidation potential values. The reduction potentials observed for $K[Ru(acs)_2]$ (−1.11 V) and [Ru(acs)(Hacs)] (−1.13 V) are very similar and much lower than the first reduction potential (−0.20 V) observed for $[Ru(Hacs)_2]ClO_4$, whereas the $Ru^{III} \rightarrow Ru^{IV}$ potentials are observed in a comparatively smaller range (0.56−0.84 V). Under identical conditions, free perchloric acid also shows a reduction response ($E_{1/2}$ = −0.25 V, ΔE_p = 100 mV). This voltammogram is very similar to that of the first reduction displayed by $[Ru(Hacs)_2]ClO_4$. The free Schiff base (H_2acs) also displays a reduction response under the same conditions. E_{pc} and E_{pa} values for this reduction response are −1.37 and −0.96 V, respectively. Considering all the above, the reductions displayed by the present series of complexes cannot be assigned to the $Ru^{III} \rightarrow Ru^{II}$ process unambiguously.

Protonation and Deprotonation of Coordinated Amide

Spectrophotometric titrations have been performed using acetonitrile solutions of $K[Ru(acs)_2]$ and CF_3SO_3H to study

the protonation behaviour of the coordinated amide functionalities in the complex. With the progressive addition of the acid the change of spectral profiles is characteristic of successive protonation of the two amide functionalities present in the two acs^{2-} ligands of $K[Ru(acs)_2]$.[2,13] The initial change in the spectral profile gradually decreases and becomes a minimum when the complex/acid mol ratio reaches 1:1.2. At this stage the spectral profile is akin to that of the neutral complex [Ru(acs)(Hacs)] indicating the protonation of the first ligand amide functionality. In this portion of the titration, the shift of band positions occurs through eight isosbestic points (455, 378, 361, 284, 250, 242, 222, and 207 nm) (Figure 7a). Continued addition of the acid causes a further shift of band positions through another set of five isosbestic points (584, 344, 374, 299, and 263 nm) (Figure 7b). The spectral profile becomes constant and similar to that of $[Ru(Hacs)_2]^+$ at a complex/acid molar ratio of about 1:2.6. Quantitative reversibility of this protonation

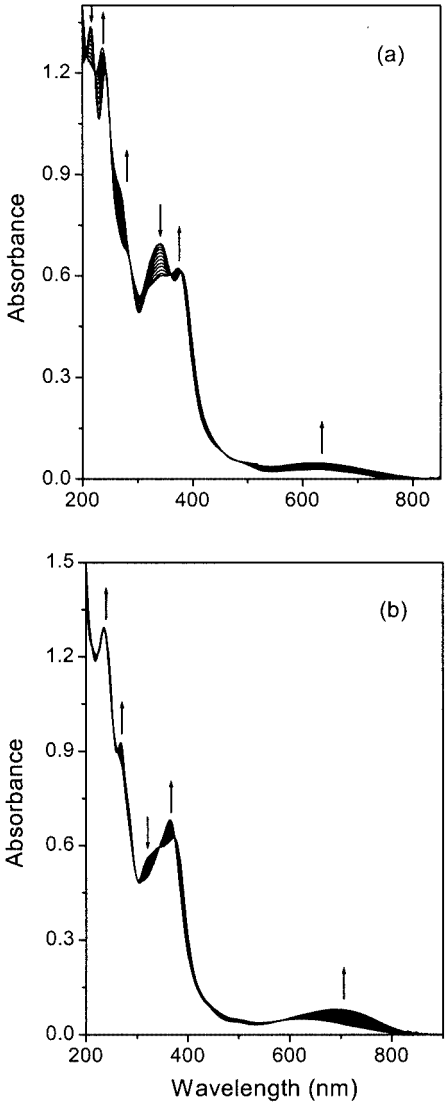

Figure 7. Spectrophotometric titration of $K[Ru(acs)_2]$ in acetonitrile with CF_3SO_3H; (a) first segment and (b) second segment of the titration (see text)

behaviour was confirmed by spectrophotometric back-titration with triethylamine. The values of pK_{a1} and pK_{a2} determined from the two segments of the titration are 6.64(4) and 7.19(1), respectively. These values are much lower than the pK_a ($\approx$15) of the free amide functionality in organic compounds.[14] This difference in the pK_a values is likely to be due to a combination of several factors. Among various explanations one possibility could be the following: the electron deficiency at the imine-N adjacent to the amide-N arising out of coordination of the former to the metal centre is compensated by the amide functionality and thereby contributes to the increase of the amide N−H acidity.[2,15] Interestingly the pK_a values determined in this work are very similar to those [pK_{a1} = 6.85(5) and pK_{a2} = 7.44(9)] determined for the ruthenium(II) complex, $[RuL_2]$, where HL is *N*-(benzoyl)-*N*′-(picolinylidene)hydrazine.[2] It seems there is no effect of the difference in the oxidation states (+3 and +2) on the acidities of the ligand amide functionalities. However, there are two very distinct dissimilarities between the two systems. In the ruthenium(II) complex, after protonation the amide functionalities are no longer bound to the metal centre which is not the case for the present complexes of acs^{2-} and $Hacs^-$ (vide supra). The ligand L^- is a pyridine-N, imine-N, and deprotonated amide-O donor whereas acs^{2-} is a phenolate-O, imine-N, and deprotonated amide-O donor. Perhaps these dissimilarities offset the effect of oxidation state on the acidity of ligand amide functionalities and similar pK_a values are observed for both systems.

Conclusion

In this article, syntheses and physical properties of three new ruthenium(III) complexes with *N*-(acetyl)-*N*′-(salicylidene)hydrazine (H_2acs) have been described. The bis complexes vary in the protonation state of the amide functionality of the ligands. The crystal structures of [Ru(acs)(Hacs)] and $[Ru(acs)_2]^-$ reveal the meridionally spanning phenolate-O, imine-N and amide-O coordinating mode of both $Hacs^-$ and acs^{2-}. In frozen solutions, all the three complexes display the typical rhombic EPR spectra for low-spin ruthenium(III) species, indicating no significant variation in the distortion pattern from octahedral symmetry of the N_2O_4 coordination spheres around the metal centre due to protonation or deprotonation of the amide functionalities. However, the potentials of the $Ru^{III} \rightarrow Ru^{IV}$ oxidation are markedly affected by the protonation state of the amide functionalities. Reversible protonation and deprotonation of the O-coordinating amide functionalities present in the ligands have been demonstrated.

Experimental Section

Materials: The Schiff base H_2acs[3a] and *cis*-$[RuCl_2(dmso)_4]$[16] were prepared by following reported procedures. All other chemicals and

solvents were of commercially available analytical grade and were used as received.

Physical Measurements: Elemental (C, H, N) analysis data were obtained with a Perkin−Elmer Model 240C elemental analyzer. Infrared spectra were collected by using KBr pellets on a Jasco-5300 FT-IR spectrophotometer. A Shimadzu 3101-PC UV/Vis/NIR spectrophotometer was used to record the electronic spectra. Room temperature solid-state magnetic susceptibilities were measured by using a Sherwood Scientific magnetic susceptibility balance. Diamagnetic corrections calculated from Pascal's constants[17] were used to obtain the molar paramagnetic susceptibilities. EPR spectra were recorded on a Jeol JES-FA200 spectrometer. Solution electrical conductivities were measured with a Digisun DI-909 conductivity meter. A CH-Instruments model 620A electrochemical analyzer was used for cyclic voltammetric experiments with acetonitrile/dimethylformamide (9:1) solutions of the complexes containing $[(n\text{-}C_4H_9)_4N]ClO_4$ (TBAP) as supporting electrolyte. The three-electrode measurements were carried out at 298 K under a dinitrogen atmosphere with a platinum disk working electrode, a platinum wire auxiliary electrode and a saturated calomel reference electrode (SCE). The potentials reported in this work are uncorrected for junction contributions.

Synthesis of the Ruthenium Complexes

[Ru(acs)(Hacs)]·H_2O: Solid *cis*-$[RuCl_2(dmso)_4]$ (242 mg, 0.5 mmol) was added to a methanol solution (40 mL) of H_2acs (178 mg, 1 mmol) and KOH (56 mg, 1 mmol). The mixture was heated under reflux for 8 h. The hot brown solution was cooled to room temperature and left in air for 5 h. The colour of the solution changed to green and the complex was precipitated as a dark green solid. It was collected by filtration, washed with methanol followed by diethyl ether and finally dried in air. The yield was 95 mg (40%). Single crystals suitable for X-ray structure determination were obtained by storing the filtrate at 5 °C for about 3−4 days.

[Ru(Hacs)$_2$]ClO_4: A methanol solution (10 mL) of 70% aqueous $HClO_4$ (0.2 mL) was prepared. To a suspension of [Ru(acs)(Hacs)]·H_2O (118 mg, 0.25 mmol) in 25 mL methanol 1 mL of the above $HClO_4$ solution was added and the mixture was magnetically stirred in air. Initially a clear green solution was obtained and after about 1/2 h a green solid separated. The complex thus obtained was collected by filtration, washed with diethyl ether and dried in air. The isolated yield was 70 mg (49%).

K[Ru(Hacs)$_2$]: [Ru(acs)(Hacs)]·H_2O (150 mg, 0.32 mmol) was dissolved in 50 mL of methanol and KOH (18 mg, 0.32 mmol) was added to the suspension. The mixture was magnetically stirred in air for 6 h. The green solution thus obtained was filtered to remove any unreacted starting complex and the filtrate was evaporated to about ca. 4−5 mL in vacuo. The green solid obtained was collected by filtration, washed with diethyl ether and dried in air. The yield obtained by this procedure was 120 mg (76%).

Spectrophotometric Titration: In a typical titration, a 3 mL aliquot of a stock solution of K[Ru(acs)$_2$] in acetonitrile {3.74×10^{-5} M, prepared by dissolving 1.84 mg (3.74 μmol) of K[Ru(acs)$_2$] in 10 mL of acetonitrile and then diluting 1 mL of this solution to 10 mL by adding the same solvent} was placed in an air-tight cuvette. Protonation of K[Ru(acs)$_2$] was performed by addition of aliquots (1 μL) of an acetonitrile solution of CF_3SO_3H [1.13×10^{-2} M, prepared by dissolving 0.5 mL (5.65 mmol) in 10 mL of acetonitrile and then diluting 0.2 mL of this solution to 10 mL by adding the same solvent] with a gas-tight syringe. Protonation was considered complete when no significant change of the electronic spectrum was observed by further addition of CF_3SO_3H solution. The effective pK_{ai} (i = 1 and 2) values were determined from the two segments (Figure 7a for pK_{a2} and Figure 7b for pK_{a1}) of the spectrophotometric titration curves using Equations (1)−(3).[2,18] The value of $K_a(CF_3SO_3H)$ in acetonitrile used to calculate the pK_{ai} values is 2.512×10^{-3}.[19] The change in absorbance at 364 nm and that at 340 nm were used to calculate K_{c1} and K_{c2}, respectively.

$$K_{ai} = K_a(CF_3SO_3H)/K_{ci} \quad (1)$$

$$K_{c1} = [Ru(Hacs)_2^+][CF_3SO_3^-]/[Ru(acs)(Hacs)][CF_3SO_3H] \quad (2)$$

$$K_{c2} = [Ru(acs)(Hacs)][CF_3SO_3^-]/[Ru(acs)_2^-][CF_3SO_3H] \quad (3)$$

Table 5. Crystallographic data

Compound	[Ru(acs)(Hacs)]·H_2O	[PPh_4][Ru(acs)$_2$]·$C_6H_5CH_3$
Empirical formula	$RuC_{18}H_{19}N_4O_5$	$RuPC_{49}H_{44}N_4O_4$
Crystal system	monoclinic	triclinic
Space group	*C*2/*c*	$P\bar{1}$
a (Å)	10.789(3)	11.910(3)
b (Å)	19.872(2)	13.437(3)
c (Å)	8.768(2)	15.227(7)
α (°)	90	91.93(3)
β (°)	103.46(3)	109.650(19)
γ (°)	90	106.50(3)
V (Å^3)	1828.2(7)	2177.7(12)
Z	4	2
$D_{calcd.}$ (g cm^{-3})	1.716	1.350
μ (mm^{-1})	0.897	0.445
Reflections collected	4178	7617
Reflections unique	4020	7617
Reflections [$I > 2\sigma(I)$]	3267	3819
Parameters	131	535
*R*1, *wR*2 [$I > 2\sigma(I)$]	0.0545, 0.1394	0.0840, 0.1913
Goodness-of-fit on F^2	1.083	1.022
Largest peak, hole [e·Å^{-3}]	1.487, −1.989	0.850, −0.361

X-ray Crystallography: X-ray data for crystals of both [Ru(acs)(Hacs)]·H_2O and [PPh_4][Ru(acs)$_2$]·$C_6H_5CH_3$ were collected on an Enraf−Nonius Mach-3 single crystal diffractometer using graphite monochromated Mo-K_α radiation (λ = 0.71073 Å) by ω-scan method at 298 K. In each case, unit-cell parameters were determined by least-squares fit of 25 reflections having 2θ values in the range 10−22°. Intensities of three check reflections were measured after every 1.5 h during the data collection to monitor the crystal stability. In both cases, there was no significant change in the intensities of the check reflections. Empirical absorption corrections were applied to both datasets based on the ψ-scans.[20] The structures were solved by direct methods and refined on F^2 by full-matrix least-squares procedures. In each case, the asymmetric unit contains one molecule of the complex and one solvent molecule. All non-hydrogen atoms having full occupancy were refined using anisotropic thermal parameters. For both molecules the methyl group H-atoms and the aromatic H-atoms were placed geometrically by using a riding model. In the case of [Ru(acs)(Hacs)]·H_2O, H-atoms attached to the water oxygen atom and the amide nitrogen atom were located in a difference map. For both structures all the H-atoms were included in the structure factor calculation at idealised positions [with U_{iso}(methyl-H) = 1.5U_{eq}(C), U_{iso}(aromatic-H) = 1.2U_{eq}(C), U_{iso}(water-H) = 1.5U_{eq}(O), and U_{iso}(amide-H) = 1.2U_{eq}(N)], but not refined. The programs of WinGX[21] were used for data reduction and absorption correction. Structure solution and refinement were performed with the SHELXL-97 programs.[22] The Ortex6a[23] and Platon98[24] packages were used for molecular graphics. Selected crystal and refinement data are listed in Table 5.

CCDC-208845 for [Ru(acs)(Hacs)]·H_2O and CCDC-208846 for [PPh_4][Ru(acs)$_2$]·$C_6H_5CH_3$ contain the supplementary crystallographic data for this paper. These data can be obtained free of charge at www.ccdc.cam.ac.uk/conts/retrieving.html [or from the Cambridge Crystallographic Data Centre, 12, Union Road, Cambridge CB2 1EZ, UK; Fax: (internat.) +44-1223/336-033; E-mail: deposit@ccdc.cam.ac.uk].

Acknowledgments

Financial assistance for this work was provided by the Department of Science and Technology (DST), New Delhi (Grant No. SP/S1/F23/99). X-ray crystallographic studies were performed at the National Single Crystal Diffractometer Facility, School of Chemistry, University of Hyderabad (funded by the DST). We thank the University Grants Commission, New Delhi for the facilities provided under the Universities with potential for excellence program. Mr. Satyanarayan Pal thanks the Council of Scientific and Industrial Research, New Delhi for a research fellowship.

[1] [1a] E. A. Seddon, K. R. Seddon, *The Chemistry of Ruthenium*, Elsevier, New York, **1984**. [1b] G. Wilkinson, R. D. Gillard, J. A. McCleverty, *Comprehensive Coordination Chemistry*, Pergamon, Oxford, **1987**, *4*, 277. [1c] B. K. Ghosh, A. Chakravorty, *Coord. Chem. Rev.* **1989**, *95*, 239. [1d] A. B. P. Lever, H. Masui, R. A. Metcalfe, D. J. Stufkens, E. S. Dodsworth, P. R. Auburn, *Coord. Chem. Rev.* **1993**, *125*, 317. [1e] V. Balzani, A. Juris, M. Venturi, S. Campagna, S. Serroni, *Chem. Rev.* **1996**, *96*, 759. [1f] S.-M. Lee, W.-T. Wong, *Coord. Chem. Rev.* **1997**, *164*, 415. [1g] L. De Cola, P. Belser, *Coord. Chem. Rev.* **1998**, *177*, 301. [1h] D. B. Grotjahn, *Coord. Chem. Rev.* **1999**, *190−192*, 1125. [1i] K. Szaciowski, W. Macyk, G. Stochel, Z. Stasicka, S. Sostero, O. Traverso, *Coord. Chem. Rev.* **2000**, *208*, 277. [1j] B.-Z. Shan, Q. Zhao, N. Goswami, D. M. Eichhorn, D. P. Rillema, *Coord. Chem. Rev.* **2001**, *211*, 117. [1k] M. J. Clarke, *Coord. Chem. Rev.* **2002**, *232*, 69. [1l] L. Sun, L. Hammarström, B. Åkermark, S. Styring, *Chem. Soc. Rev.* **2001**, *30*, 36. [1m] P. D. Beer, *Acc. Chem. Res.* **1998**, *31*, 71. [1n] N. Sardesai, S. C. Lin, K. Zimmermann, J. K. Barton, *Bioconjugate Chem.* **1995**, *6*, 302. [1o] H. B. Grey, J. R. Winkler, *Annu. Rev. Biochem.* **1996**, *65*, 537. [1p] P. Lincoln, E. Tuite, B. Nordén, *J. Am. Chem. Soc.* **1997**, *119*, 1454. [1q] S. Goswami, A. R. Chakravarty, A. Chakravorty, *J. Chem. Soc., Chem. Commun.* **1982**, 1288. [1r] J. A. Gilbert, D. S. Eggleston, W. R. Murphy, Jr., D. A. Geselowitz, S. W. Gersten, D. J. Hodgson, T. J. Meyer, *J. Am. Chem. Soc.* **1985**, *107*, 3855. [1s] C.-M. Che, *Pure Appl. Chem.* **1995**, *67*, 225. [1t] T. Naota, H. Takaya, S.-I. Murahashi, *Chem. Rev.* **1998**, *98*, 2599.

[2] S. N. Pal, S. Pal, *J. Chem. Soc., Dalton Trans.* **2002**, 2102.

[3] [3a] S. C. Chan, L. L. Koh, P. -H. Leung, J. D. Ranford, K. Y. Sim, *Inorg. Chim. Acta* **1995**, *236*, 101. [3b] N. R. Sangeetha, C. K. Pal, P. Ghosh, S. Pal, *J. Chem. Soc., Dalton Trans.* **1996**, 3293. [3c] S. P. Rath, S. Mondal, A. Chakravorty, *Inorg. Chim. Acta* **1997**, *263*, 247. [3d] N. R. Sangeetha, S. Pal, *Bull. Chem. Soc. Jpn.* **2000**, *73*, 357. [3e] M. R. Maurya, S. Khurana, C. Schulzke, D. Rehder, *Eur. J. Inorg. Chem.* **2001**, 779.

[4] [4a] D. W. Margerum, *Pure Appl. Chem.* **1983**, *55*, 23. [4b] K. L. Kotska, B. G. Fox, M. P. Hendrich, T. J. Collins, C. E. Pickard, L. J. Wright, E. Münck, *J. Am. Chem. Soc.* **1993**, *115*, 6746. [4c] M. Mikuriya, D. Jie, Y. Kakuta, T. Tokii, *Bull. Chem. Soc. Jpn.* **1993**, *66*, 1132.

[5] W. J. Geary, *Coord. Chem. Rev.* **1971**, *7*, 81.

[6] [6a] R. M. Silverstein, F. X. Webster, *Spectrometric Identification of Organic Compounds*, Wiley, New York, **1998**, 6th ed., p 101. [6b] K. Nakamoto, *Infrared and Raman Spectra of Inorganic and Coordination Compounds*, Wiley, New York, **1986**, 4th ed., p 228.

[7] F. Basuli, A. K. Das, G. Mostafa, S.-M. Peng, S. Bhattacharya, *Polyhedron* **2000**, *19*, 1663.

[8] [8a] B. Bleany, M. C. M. O'Brien, *Proc. Phys. Soc., London, Sect. B* **1956**, *69*, 1216. [8b] J. S. Griffith, *The Theory of Transition Metal Ions*, Cambridge University Press, London, **1961**, p. 364. [8c] S. Bhattacharya, A. Chakravorty, *Proc. Indian Acad. Sci. (Chem. Sci.)* **1985**, *95*, 159.

[9] [9a] S. N. Pal, S. Pal, *Inorg. Chem.* **2001**, *40*, 4807. [9b] A. K. Das, S. -M. Peng, S. Bhattacharya, *J. Chem. Soc., Dalton Trans.* **2000**, 181. [9c] B. Mondal, S. Chakraborty, P. Munshi, M. G. Walawalkar, G. K. Lahiri, *J. Chem. Soc., Dalton Trans.* **2000**, 2327. [9d] K. Nakajima, Y. Ando, H. Mano, M. Kojima, *Inorg. Chim. Acta* **1998**, *274*, 184. [9e] S. Pattanayak, K. Pramanik, N. Bag, P. Ghosh, A. Chakravorty, *Polyhedron* **1997**, *16*, 2951.

[10] H. Miyasaka, H.-C. Chang, K. Mochizuki, S. Kitagawa, *Inorg. Chem.* **2001**, *40*, 3544.

[11] [11a] M. Nishio, Y. Umezawa, M. Hirota, Y. Takeuchi, *Tetrahedron* **1995**, *51*, 8665. [11b] K. S. B. Hancock, J. W. Steed, *Chem. Commun.* **1998**, 1409. [11c] K. Biradha, M. J. Zaworotko, *J. Am. Chem. Soc.* **1998**, *120*, 6431.

[12] $E_{1/2}$ = (E_{pa} + E_{pc})/2, ΔE_p = E_{pa} − E_{pc} where E_{pa} and E_{pc} are anodic and cathodic peak potentials. Scan rate is 50 mVs^{-1}.

[13] [13a] C. Long, J. G. Vos, *Inorg. Chim. Acta* **1984**, *89*, 125. [13b] S. Baitalik, U. Flörke, K. Nag, *Inorg. Chem.* **1999**, *38*, 3296.

[14] D. D. Perrin, B. Dempsey, E. P. Serjeant, *pK_a Prediction for Organic Acids and Bases, Chapman and Hall, London and New York,* **1981**.

[15] B. Mondal, S. Chakraborty, P. Munshi, M. G. Walawalkar, G. K. Lahiri, *J. Chem. Soc., Dalton Trans.* **2000**, 2327.

[16] I. P. Evans, A. Spencer, G. Wilkinson, *J. Chem. Soc., Dalton Trans.* **1973**, 204.
[17] W. E. Hatfield, *Theory and Applications of Molecular Paramagnetism* (Eds.: E. A. Boudreaux, L. N. Mulay), Wiley, New York, **1976**, p. 491.
[18] C. E. Dubé, D. W. Wright, S. Pal, P. J. Bonitatebus, Jr., W. H. Armstrong, *J. Am. Chem. Soc.* **1998**, *120*, 3704.
[19] K. Izutsu, *Acid-Base Dissociation Constants in Dipolar Aprotic Solvents*, Blackwell, Oxford, **1990**, p. 28.
[20] A. C. T. North, D. C. Philips, F. S. Mathews, *Acta Crystallogr., Sect. A* **1968**, *24*, 351.
[21] L. J. Farrugia, *J. Appl. Crystallogr.* **1999**, *32*, 837.
[22] G. M. Sheldrick, *SHELXL-97, Programs for Structure Determination and Refinement*, University of Göttingen, Göttingen, Germany.
[23] P. McArdle, *J. Appl. Crystallogr.* **1995**, *28*, 65.
[24] A. L. Spek, *Platon98, Molecular Graphics Software*, University of Glasgow, UK, **1998**.

Received April 23, 2003
Early View Article
Published Online October 2, 2003

